



## *Effect of Shape of Twin Tunnels during Seismic Loading*

*S.D.Anitha Kumari<sup>a,\*</sup>, K.S. Vipin<sup>b</sup>, T.G. Sitharam<sup>a</sup>*

<sup>a</sup>*Dept of Civil Engg., Indian Institute of Science, Bengaluru, India*

<sup>b</sup>*SwissRe Shared Services, Bengaluru, India*

*\*Corresponding author: [anitha.vipin@gmail.com](mailto:anitha.vipin@gmail.com)*

### **ABSTRACT**

The demand for more effective transportation in the fast developing tier two cities in India has led to the construction of underground tunnels. To understand the mechanical behaviour of these structures, elasto-plastic dynamic numerical modelling is preferred. In this study, twin tunnels with circular and horse-shoe cross section is modelled to understand the effect of the shape of the tunnel. In addition to this, the effect of varying shallow overburden on the mechanical response in case of the two cross-sections is also presented. The study indicates that under uniform overburden thickness, the stress distributions were not affected by the shape of the tunnel. However in the case of non-uniform thickness, the circular section was subjected to more stresses compared to the horse-shoe section. The distribution of the bending moment, shear forces and axial forces on the horse-tunnel lining was found to be more compared to that of the circular cross-section. However the distribution of bending moment was more uniform in the case of horse-shoe section.

**Keywords:** Twin tunnels; Seismic loading; Tunnel shapes; Finite element method

### **1. INTRODUCTION**

Rapid modernization and the requirement of proper infrastructural facilities have pushed the demand for more effective transportation in the fast developing Indian cities. In this context, underground twin tunnels (Closely spaced tunnels running adjacent to each other either side by side or below/above one another) are a viable solution in congested urban areas. The underground tunnels generally help to avoid surface congestion and reduce atmospheric pollution. Some of the examples of underground tunnels include railway tunnels, highway tunnels, sewerage tunnels, water tunnels etc. These tunnels can be of different shapes like circular, rectangular, elliptical, D or horse-shoe. The tunnels are generally excavated in weak/strong rock masses or soft ground depending upon the requirement. Horse-shoe shaped tunnels are preferred in rock masses as they provide a much better arch action in resisting the load. Recent earthquakes in various parts of the world have enlightened the scientific community to understand more about the behaviour of these underground tunnels during such natural disasters. In this study a comparison of the mechanical response of twin tunnels with circular and horse shoe section under seismic condition is presented using two dimensional finite element method. It is also observed that in hilly terrain it is impossible to provide tunnels under uniform soil/rock mass cover. This emphasizes the requirement of a study to understand the behaviour of twin tunnels under varying overburden thickness and hence this aspect is also considered in this research.

## **2. MODEL STUDIES**

Two closely spaced tunnels are generally referred to as twin tunnels. These can be placed either one above the other or running side-by-side. When two tunnels are constructed close by, there is possibility that the zones of influence may overlap. But previous researches (Chen et al., 2009; Chehade & Shahrour, 2008) have shown that when the pillar width is greater than 2D, the influence is minimal. Hence in this study, the pillar width is adopted 2D and more to avoid interference from the presence of adjacent structures in stresses and strains. It is always better to model the interaction between underground openings as three-dimensional, since those studies will provide accurate results. But the complexities associated with 3D modelling generally restrict us to model using 2D plain strain conditions. However, two-dimensional elasto-plastic analysis is sufficient to understand the distribution of stresses and strains around openings and hence a two-dimensional elasto-plastic analysis is used for the present study.

## **3. NUMERICAL SIMULATIONS**

Numerical simulations adopting two dimensional plane-strain analysis is performed using PLAXIS software. Generally circular tunnels are preferred over other shapes in numerical simulation because of the simplicity in modelling. But in practice, horse-shoe shaped/D-shaped tunnels are found to be more convenient than circular tunnels. In this study, a comparative behaviour of the tunnels with different shapes is done by modelling circular and horse-shoe shaped twin tunnels. The effect of varying overburden depth above the tunnel is also presented to understand the variation in the displacements and stresses around the tunnel opening. The horse-shoe shaped tunnel is having a horizontal dimension of 12m and vertical height of 9m. The circular shaped tunnel model is having a diameter of 10m.

Tunnels can be aligned horizontally or vertically (piggy back). In this study, the tunnels are aligned side-by-side (horizontally). The crowns of both the tunnels are at a depth of 8m from the ground surface. The pillar width is kept as 22m which is more than 2 times the effective diameter of the tunnels considered. This will help to reduce the interference caused by the presence of adjacent structures. The bottom boundary from the invert of the tunnel is at a depth of 14/15m and the clear distance to the boundaries are provided at 23/24m to avoid the boundary effects. To simulate the earthquake loading, strong motion data from USGS (2011), is used in this study. While modelling, the boundary conditions along the vertical walls are modelled as absorbent to prevent the reflection of the seismic waves into the model. In addition to this, the boundary effects will be minimal in the simulation. The boundary conditions of the vertical walls are given such that the displacements along the horizontal direction is fixed where as the vertical direction is free. The bottom boundary is fixed against horizontal and vertical movements. The top boundary representing the ground surface is free so that settlements are not restricted. Drained conditions are used for the analysis. The real soil behaviour can be approximated by the elastic-perfectly plastic Mohr-Coulomb model and it requires only minimum basic input parameters viz. Young's modulus, Poisson's ratio, cohesion, friction angle and dilatancy angle.

The general steps involved in PLAXIS modelling are:

- (i) definition of the geometry,
- (ii) meshing of the geometry,
- (iii) selection of appropriate models for the analysis and the input of material properties and
- (iv) initial and boundary conditions of the model.

Figure 1 shows the meshed model of twin tunnels with two different shapes of the tunnel sections. While meshing, fifteen noded triangular elements are used. Finer meshes are preferred as they provide higher accuracy, but may increase the computational time and hence generally fine meshes

are provided only around the openings and medium meshes are provided at farther ends. The model consists of 394 elements with 3341 nodes and the average element size of the mesh is 2.7m. Table 1 shows the properties used for the soil mass or very weak rock mass. A thickness of 0.5m was given to the tunnel lining. The properties of the tunnel lining adopted for this study is given in Table 2. Tunnel linings are also significant as they should also be designed for withstanding both static and dynamic loads (Duhee et al., 2009).

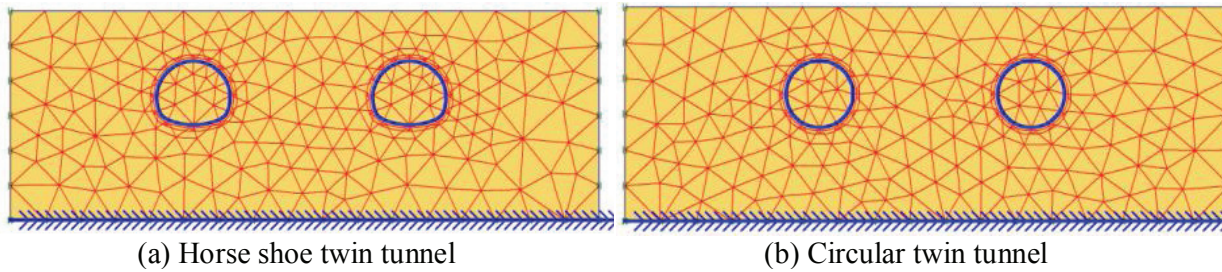


Fig. 1 - Horseshoe/circular twin tunnels modelled for the study

Table 1 - Properties of the soil/very weak rock mass

Material model & Type	Mohr-Coulomb, drained
Saturated density	20 kN/m <sup>3</sup>
Dry density	17 kN/m <sup>3</sup>
Permeability, k <sub>h</sub>	1m/day
Permeability, k <sub>v</sub>	1m/day
Young's modulus	40000 kN/m <sup>2</sup>
Poisson's ratio	0.3
Cohesion	50kN/m <sup>2</sup>
Friction angle	32°
Dilatancy angle	2°

Table 2 - Properties of the tunnel lining

Property	Value
EA	1.4e7 kN/m
EI	1.43e5 kN/m
D	0.35m
Weight	8.4 kN/m/m
Poisson's ratio	0.15

Once the model is meshed, gravity loading is applied to the model in the first stage.  $K_0$  procedure is adopted for generating the initial stresses in the system where  $K_0$  is calculated as  $K_0 = 1 - \sin\phi$ . This is followed by the excavation of tunnels which leads to the redistribution of stresses around the tunnels. The excavation is simulated such that both the tunnels are excavated simultaneously. Finally the earthquake loading is applied to the model and the response of the system under different conditions is studied. The strong motion data used for the earthquake loading in the case of uniform and non-uniform overburden thickness is shown in Fig. 2. From this data, it was found that for a sample rate of 200, the acceleration record is having a maximum peak horizontal acceleration value of 0.2 g. For simulating this condition, the acceleration was applied at the bottom of the model.

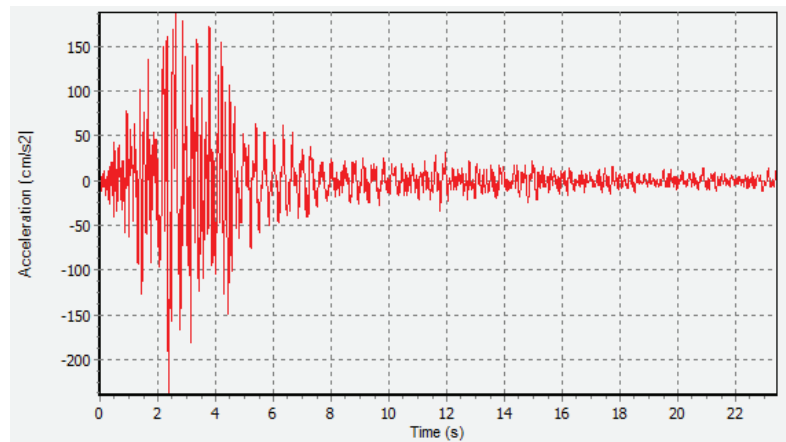


Fig. 2 - Strong motion data used for the analysis (USGS, 2011)

#### 4. RESULTS AND DISCUSSIONS

Figure 3 shows the stress distributions around the twin tunnels with uniform overburden. As expected it can be seen that the stresses increase as the overburden thickness increases. The stresses on the crown of the horseshoe shaped tunnel are slightly higher than the circular tunnels and are distributed over a larger area. But the concentration of stresses on the left and right sides along the spring line of both the tunnels are almost similar for the considered sections. In addition, the stress distribution in between the tunnels is also found to be uniform irrespective of the shape of the tunnel.

To compare the variation in the stress distribution due to varying overburden thickness, another section was modelled and the corresponding distribution is shown in Fig. 4. It can be seen from this figure that more stresses are concentrated towards the right spring line of the right tunnels in both the cases. Also it can be seen that in case of the circular section of tunnels, there is a larger stress concentration towards the higher overburden side compared to that of the section with horseshoe shape. This indicates that when the overburden thickness is varying as observed in most field cases, there is better redistribution of stresses in non-circular tunnels. Moreover, the stress contours clearly indicate that the soil/very weak rock mass layers below the tunnels are highly stressed in the case of circular cross section tunnels when compared to that of the horse-shoe shaped tunnels. The stress distribution at the invert of the non-circular tunnels indicates the magnitude is less than that of circular tunnels.

The displacement vector plot as shown in Fig. 5 indicates that the horse-shoe section is having an extreme displacement of 90mm whereas the circular section is having a total extreme displacement of 91mm under the given earthquake loading. This indicates that the magnitude of extreme values of total displacement is same for both the cross sections. However the distribution of the displacement around the tunnel was slightly different for both the sections. The horseshoe section indicated that the displacement is more towards the right side of the spring line whereas in the case of the circular section, the vector was thicker in the left spring line. The net displacement was found to be uniform along the spring line and the crown, but with higher intensity surrounding these regions indicating higher movements near the tunnel. An analysis of the vertical displacement showed that it is maximum near the crown of the tunnel, but minimum at the invert. Figure 6 shows the distribution of the displacement vectors when the overburden is of varying thickness. In this case there was marked difference in the magnitude observed for the total displacement for the horseshoe tunnel section and circular section. The extreme displacement for horse-shoe section is 206mm whereas under the same conditions for a circular section it is seen to be 343mm. Both these

values are significantly higher compared to the magnitude of 90mm obtained when the tunnel sections were under a uniform overburden. It is also observed that there is considerable amount of heave along the edge of the slope for both the sections and the heave is more predominant for circular section model.

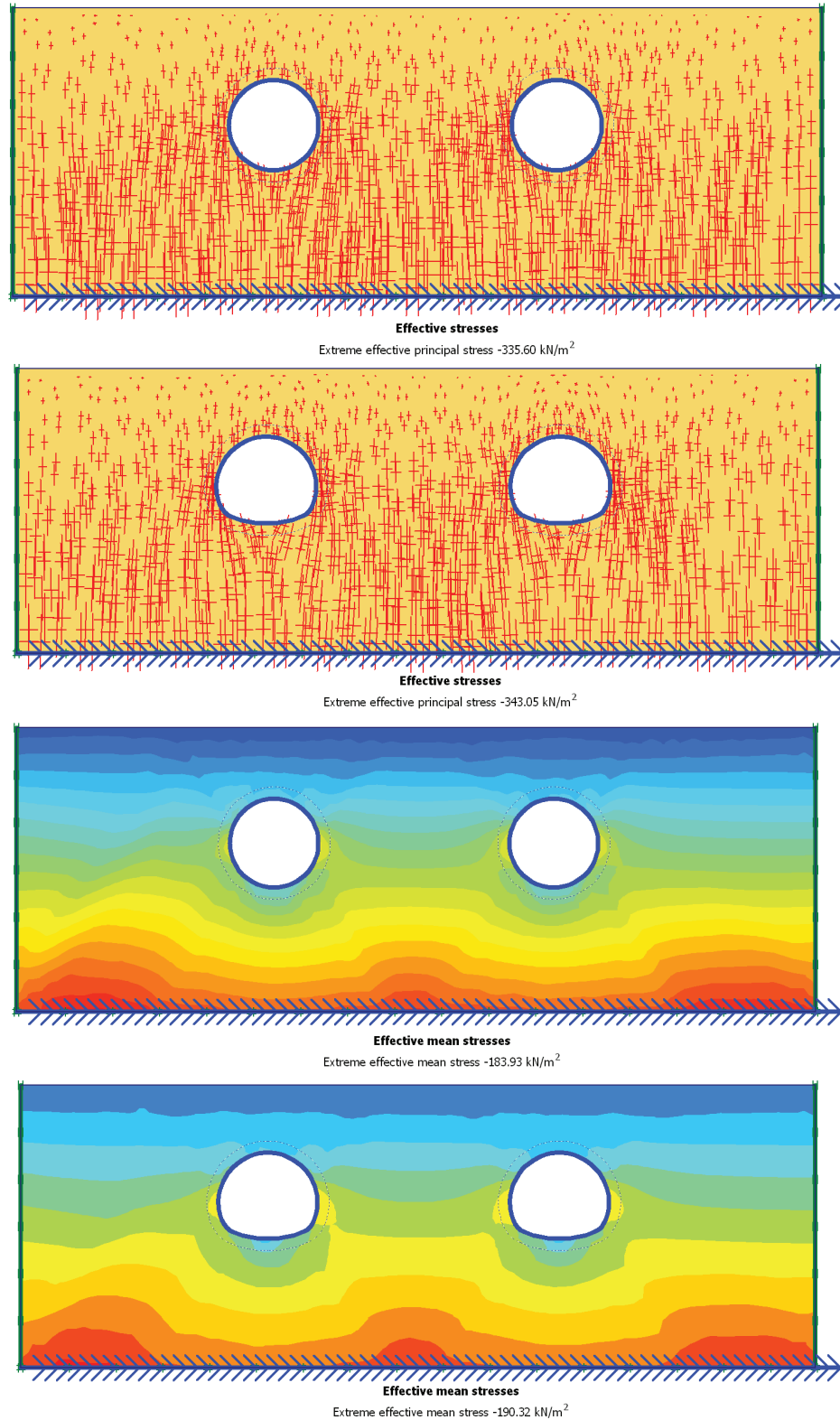


Fig. 3 - Stress distribution around the tunnels with uniform overburden thickness

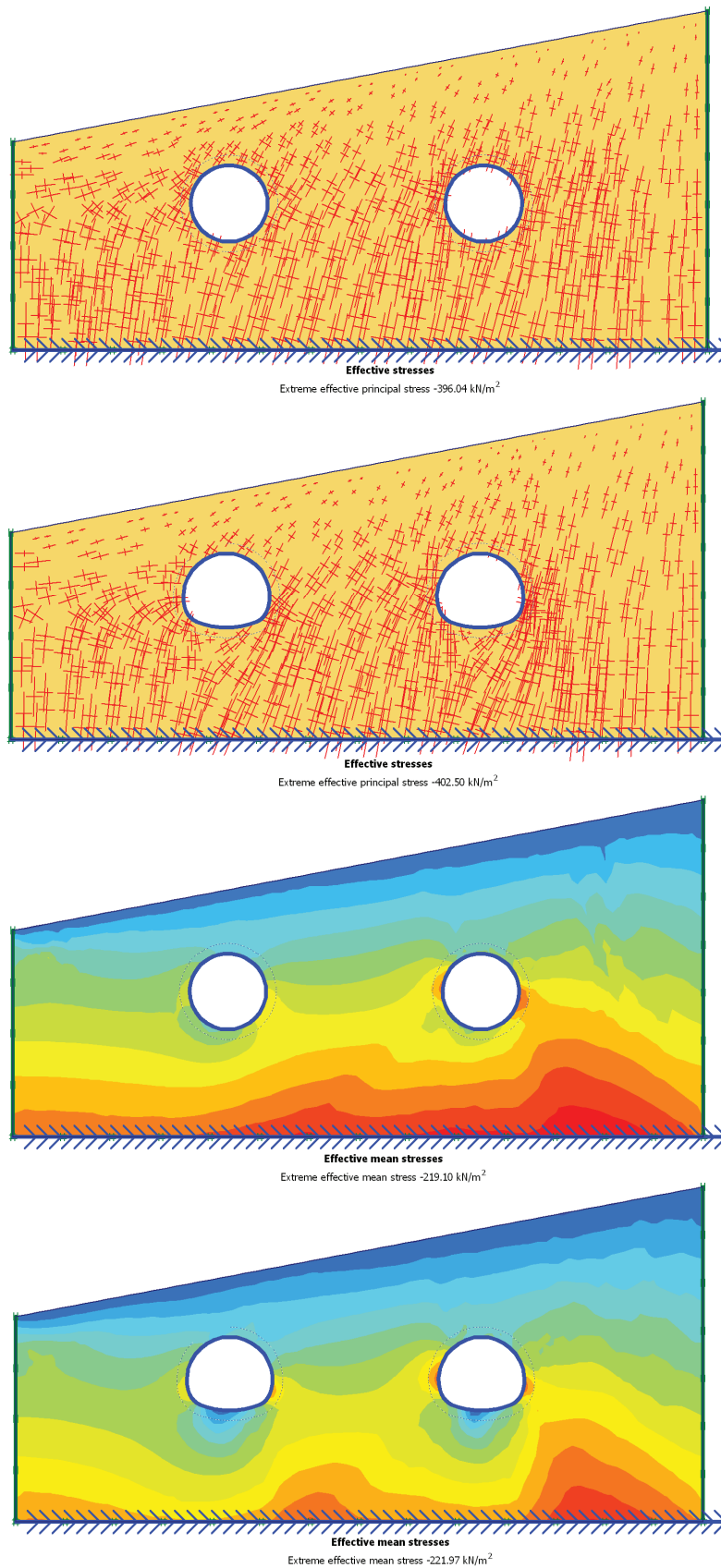


Fig. 4 - Stress distribution around the tunnels with varying overburden thickness

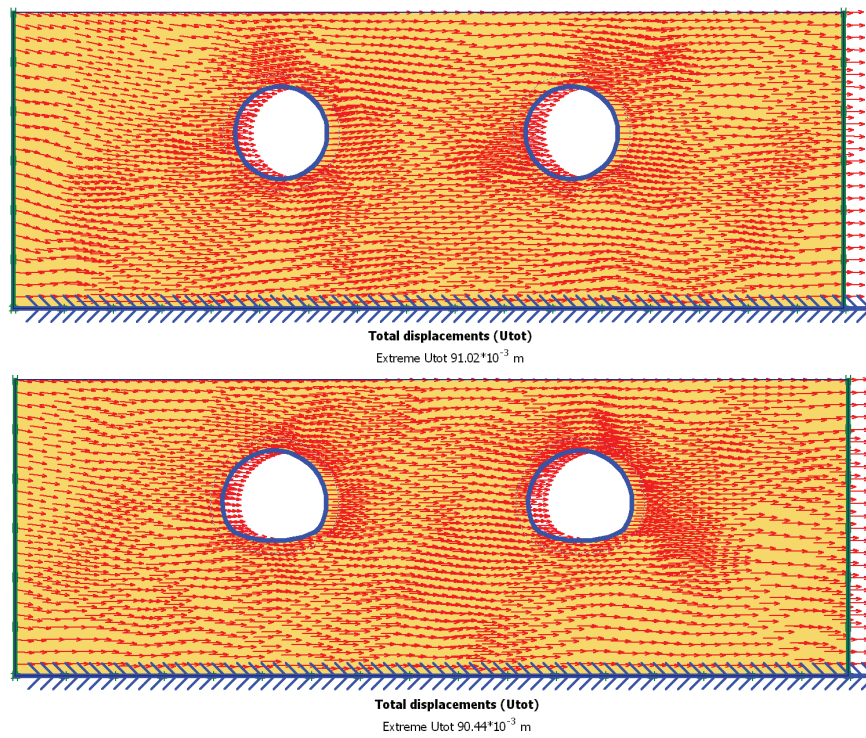


Fig. 5 - Total Displacement vectors when overburden is of uniform thickness

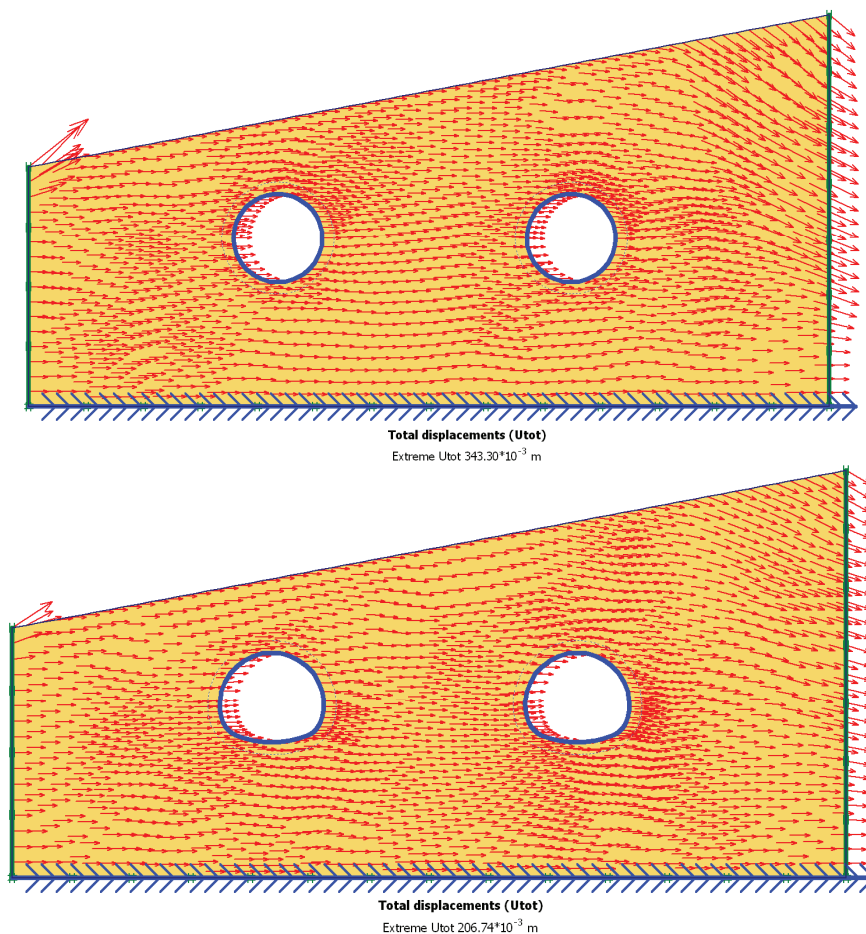


Fig. 6 - Total displacement vectors when overburden is of varying thickness

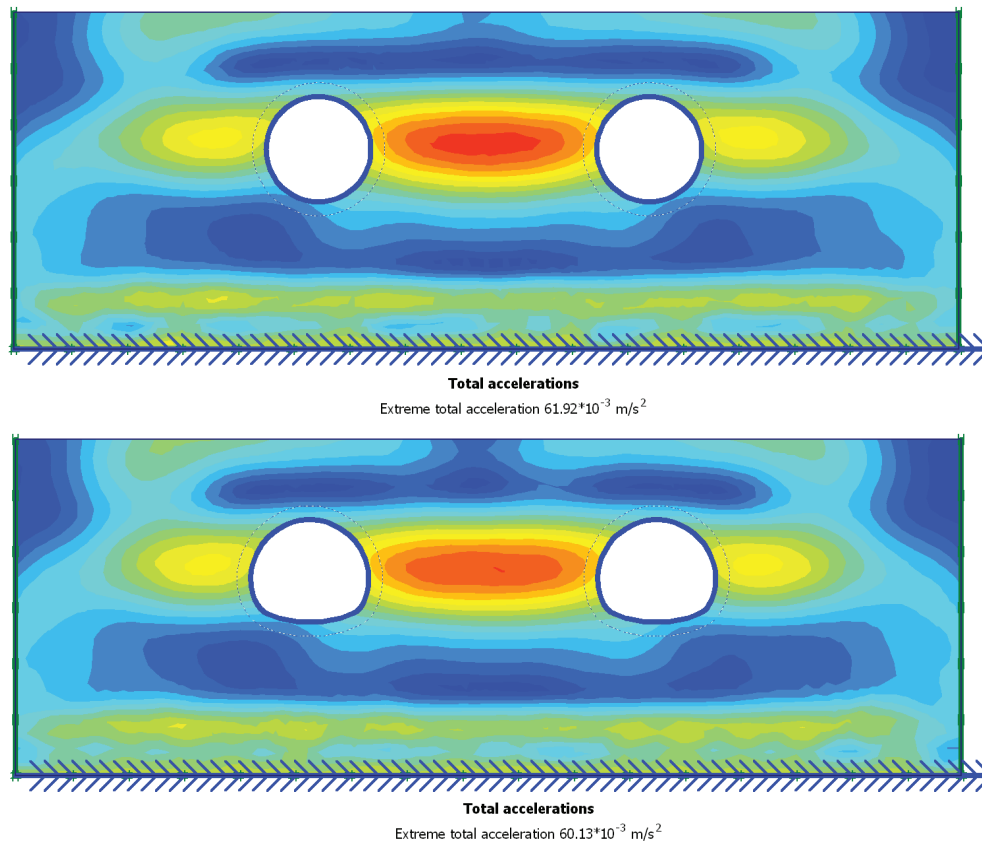


Fig. 7 - Total acceleration distribution when overburden is of uniform thickness

Figures 7 and 8 show the variation of total acceleration when the overburden is of uniform and varying thickness. It can be seen that in the case of uniform overburden the variation of acceleration was uniform along the spring line with maximum distribution in between the tunnels. But in the case of varying shallow overburden thickness, it can be seen that towards the higher overburden side, the magnitude of acceleration is comparatively less for both the cases. Moreover, there is a reduction in the magnitude of the acceleration in this case which can be seen from the contour shadings. The maximum acceleration for circular tunnels with uniform and non-uniform overburden thickness are  $61 \text{ mm/s}^2$  and  $47 \text{ mm/s}^2$  respectively whereas for the horse-shoe tunnels it is  $60 \text{ mm/s}^2$  and  $48 \text{ mm/s}^2$  respectively which indicates that the magnitude of acceleration remains same irrespective of the shape of the tunnel. However there is significant variation in the distribution of accelerations when the variation of overburden thickness is considered. It is observed that there is a drastic reduction in the acceleration on the extreme right spring line portion where the overburden thickness is high. When the thickness was uniform, the distribution of acceleration along the left and right spring lines of both the tunnels was also uniform with a slightly higher magnitude for the circular tunnels.

Figure 9 shows the variation of the bending moments for the two different tunnel lining sections. It is observed that for both the left and right tunnels, the horse shoe section is having more bending moment values compared to that of the circular sections. The maximum bending moment is seen on the left tunnel and along the left spring line and is having magnitude of  $223 \text{ kN/m}$  and  $306.37 \text{ kN/m}$  for circular and horse-shoe sections respectively. However the maximum moment observed for the right tunnel is slightly lesser than the left one and moreover the distribution for the right tunnel is

almost uniform along the left and right spring lines. In the case of horse shoe shaped tunnels it is observed that the distribution of bending moment has become more spread out which is attributed to the more curved profile of the lower part of the tunnel. The magnitude of maximum bending moments in the case of horse-shoe shaped tunnels is 37% and 46% higher for the left and right tunnels respectively when compared with the circular twin tunnels. However when the two horse shoe shaped tunnels are compared there is not much significant changes in the distribution of bending moment around the tunnels. This indicates that the load is equally shared between the tunnels. As reported by Kim et al. (1998), it is also observed that the maximum bending moments are at the spring line regions. Also it is observed that the moment distribution is symmetrical for the circular as well as horse-shoe shaped sections. Similar to the observations made in bending moments, a comparison of the shear forces of the two sections indicates that the values are higher for the horse-shoe shaped section with values around 1.17 and 1.42 times higher than the respective circular sections as shown in Fig.10.

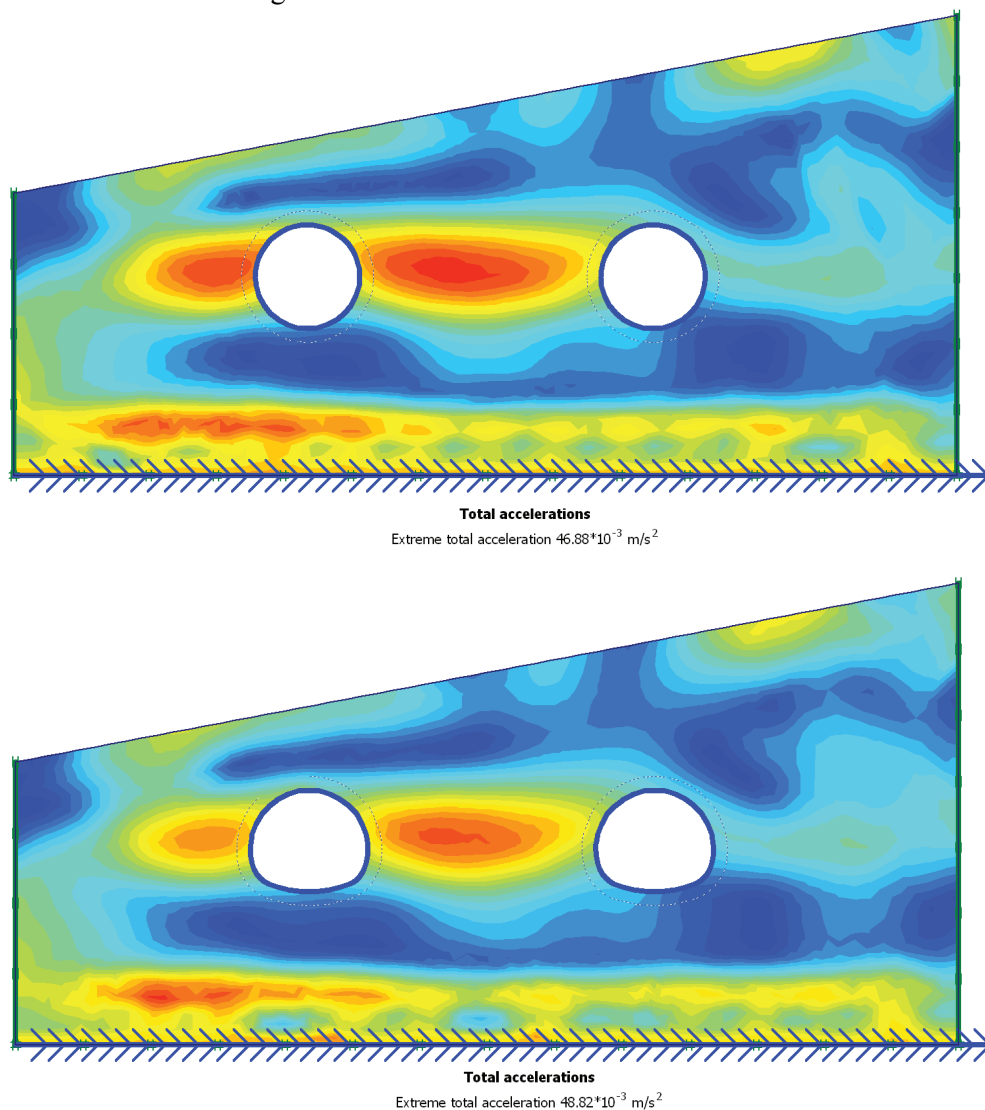


Fig. 8 - Total acceleration distribution when overburden is of varying thickness

A closer examination into the magnitudes at various nodes indicates that the axial force values at the crown and the invert are the minimum as seen in Fig. 11. It is also found that in the case of the left tunnel, the maximum axial force capacity is observed along the left spring line whereas in the case of right tunnel, the highest value is observed towards the right spring line. This indicates that even though the tunnels are placed at a conservative pillar width, there is influence of the presence

of one structure on the load carrying capacity of the other. However the axial forces are slightly higher for the horseshoe section but compared to the bending moment and shear force increments, the values are just around 5% higher than the corresponding circular sections.

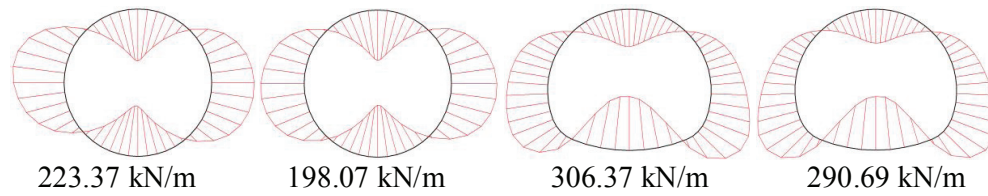


Fig. 9 - Variation of maximum bending moments in the twin tunnels with uniform overburden

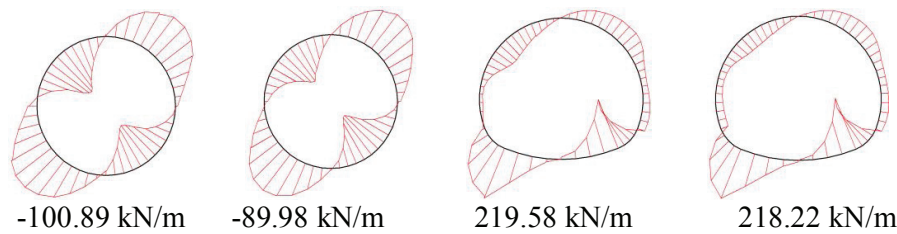


Fig. 10 - Variation of maximum shear forces in the twin tunnels with uniform overburden

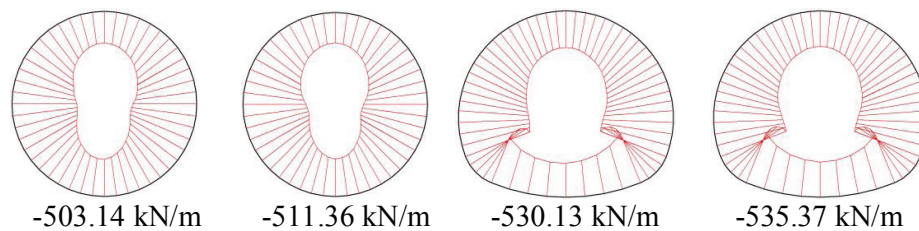


Fig. 11 - Variation of maximum axial forces in the twin tunnels with uniform overburden

Figures 12, 13 and 14 show the variation of bending moments, shear forces and axial forces respectively on the tunnel lining of circular twin tunnels and horse-shoe twin tunnels when the overburden thickness varies above the tunnels. It can be seen that the tunnel lining under the deeper cover is experiencing higher vertical stresses which is translated as higher bending moment magnitudes and the distribution pattern also changes indicating redistribution of the moments when the overburden thickness changes. It is observed that in the case of horse-shoe shaped tunnels, the invert is subjected to maximum bending compared to that of the crown. When the left and right tunnels are considered, the right tunnels are having higher magnitudes of bending moments, shear and axial forces. Also it is observed that there is a shift in the regions where the maximum values are seen.

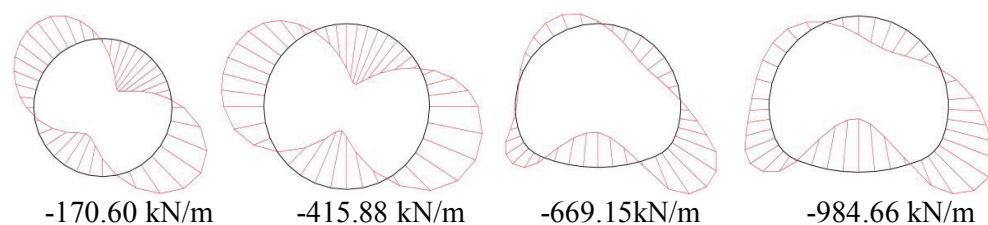


Fig. 12 - Variation of maximum bending moments in the twin tunnels with varying overburden

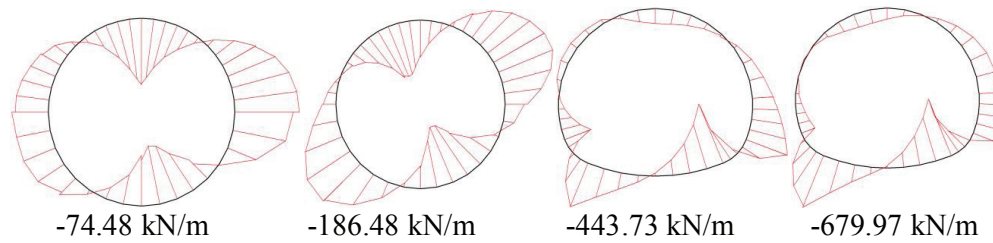


Fig. 13 - Variation of maximum shear forces in the twin tunnels with varying overburden

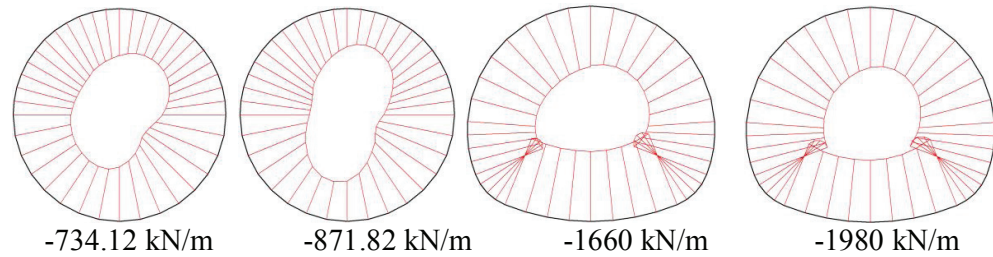


Fig. 14 - Variation of maximum axial forces in the twin tunnels with varying overburden

## 5. CONCLUSIONS

A dynamic elasto-plastic analysis of the effect of shape on the behaviour of the twin tunnels indicates that the shape has not much effect when the tunnels are subjected to uniform overburden depth. However, when the tunnels are constructed under varying shallow overburden depth, horse-shoe sections are found to be more suitable than the circular sections. This is because the arch action offered by the horse shoe sections resulted in a more uniform distribution of stresses and less heave. The distribution of stresses around the horse-shoe sections are found to be more uniform compared to that of the circular sections. The amount of heave observed in the case of circular tunnels when the overburden was non-uniform is around 1.7 times higher than that of horse-shoe shaped tunnels.

## References

- Chen, S. L., Lee, S.C. and Gui, M.W. (2009). Effects of rock pillar width on the excavation behavior of parallel tunnels, *Tunneling and Underground Space Technology*, 24, pp 148-154.
- Cehade, Hage F. and Shahrour, I. (2008). Numerical analysis of the interaction between twin tunnels: Influence of the relative position and construction procedure, *Tunneling and Underground Space Technology*, 23, pp. 210-214.
- Duhee, Park, Myung Sagong, Dong-Yeop Kwak and Chang-Gyun Jeong (2009). Soil dynamics and earthquake engineering, Vol 29(11-12), pp. 1417-1424.
- Kim, S.H., Burd, H.J., and Milligan, G.W.E. (1998). Model testing of closely spaced tunnels in clay, *Géotechnique*, 48(3), pp. 375-388.
- USGS (2011). [http://nsmpr.wr.usgs.gov/data\\_sets/upland.html](http://nsmpr.wr.usgs.gov/data_sets/upland.html).